CALIBRATION ACCURACY OF AERIAL MULTISPECTRAL REFLECTANCE IMAGES AND ESTIMATION OF ERROR SOURCES

André ROTHKIRCH, Martin KOLLEWE and Hartwig SPITZER
II. Institute for Experimental Physics, University of Hamburg, Germany
Mail: A. Rothkirch / KOGS, Vogt-Kölln-Str. 30, 22527 Hamburg, FRG
WWW-Page: http://kogs-www.informatik.uni-hamburg.de/projects/censis/remotesens.html
E-mail: rothkirc@kogs.informatik.uni-hamburg.de

ABSTRACT:

We have performed a systematic study of the calibration accuracy of multispectral aerial reflectance images. The study is part of the improvement of change detection for aerial and satellite multispectral images. It is based on (a) a multitemporal image data set from the multispectral airborne scanner Daedalus AADS 1268 and (b) simultaneously made ground based hyperspectral reflectance measurements. Reflectance images were obtained from the raw images by processing with the program package SENSAT-5, using standard urban atmospheres in the MODTRAN code. The systematic uncertainty of the resulting reflectance spectra is mainly due to the uncertainty in the atmospheric parameters. It can be reduced by fitting the Daedalus spectra to ground truth hyperspectral reflectance measurements of selected surfaces. The resulting uncertainty σ_ρ/ρ of the reflectance ρ is estimated to be 11.0 % on average.

KEY WORDS: Remote sensing, Reflectance, Error sources

1 INTRODUCTION

Remotely sensed multitemporal images are usually taken under different illumination conditions and observation geometries. In order to be independent of such influences, a transformation of the measured radiances into reflectances is a prerequisite for change detection [Wiemker et al., 1997]. This transformation can be done in two ways: by radiative transfer models and by ground truth (independent reflectance measurements). Using radiative transfer models one needs to have precise information on atmospheric conditions, which in practice is often not available. Therefore the reflectance accuracy is limited by the simulation of the atmosphere. Moreover errors in sensor radiance calibration affect the calculated reflectances. The second approach is to measure the reflectance at selected ground control points at the time as the remotely sensed image (alternatively reference planes with known reflectance characteristics can be displayed during overflights). In this study we apply both approaches in order to estimate the accuracy of the resulting multispectral reflectance spectra.

2 MEASUREMENTS

2.1 Overflights and ground based measurements

Overflights took place over Nürnberg, FRG (airport, industrial park, residential area and nature reserve) on August 26, 1997. The overflights were done at altitudes of 300m (06:57h to 07:50h and 11:01h to 11:51h UT) and 900m (10:22 to 10:48 UT). All data sets were recorded with the

11-channel airborne scanner Daedalus AADS 1268, operated by the German Aerospace Research Establishment (DLR), Oberpfaffenhofen, FRG.
Ground based measurements of the spectral reflectance were made at selected locations simultaneously with the overflights. Reflectance spectra were obtained using the 870 channel (0.4 - 2.5 μm) spectroradiometer IRIS of Bundesamt für Geowissenschaften und Rohstoffe (BGR), Hannover, FRG. Measurements were taken at five target areas of approximately 0.01 m^2 each. The chosen ground coverings were: 1) concrete (airport runway), 2) asphalt (airport), 3) artificial lawn (soccer field), 4) natural lawn (soccer field), 5) asphalt (industrial park). Reflectances of areas 1, 2 and 5 were used for a recalibration of the Daedalus reflectances. Areas 3 and 4 were used to check the result.

3 ACCURACY OF DAEDALUS REFLECTANCE SPECTRA

Daedalus based reflectances were determined in two steps. For each pixel (scan angle θ) and each channel Daedalus spectral radiances $L_M(\theta)$ were calculated from grey levels, the gain factor and a calibration at the Daedalus-testbench (laboratory). In parallel, radiances $L_S(\theta, \rho_D)$ as a function of ground reflectance ρ_D were simulated with the radiative transfer model (SENSAT/MODTRAN, [Anderson et al., 1995], [Richter, 1994]). ρ_D is determined by comparing $L_M(\theta)$ and $L_S(\theta, \rho_D)$ ('inverse modelling'). See [Hepp-94], [Richter, 1994] for details.

3.1 Noise of the Daedalus-detector

The calibration of the Daedalus detector was performed by DLR after the overflight. Scan frequencies of 12.5 , 25, 50 and 100 Hz where chosen. The Daedalus scanner was mounted on a calibration bench, a constant radiance illuminated the scanner optics. 100 lines where recorded for each scan frequency. The calibration factor C is defined by the linear relationship between the scanner signal D_{cal} (minus the dark-current D_0) and the radiance L_{cal} of the calibration source:

$$C = L_{cal}/(D_{cal} - D_0) \tag{1}$$

The *noise equivalent radiance* L_{NE} for each channel, a measure of the instrumental noise, is defined by using the standard deviation of the dark-current measurements σ divided by the gain factor γ:

$$L_{NE} = C \cdot \sigma/\gamma \tag{2}$$

The noise is assumed to be additive. Thus, the relative accuracy F_D of the Daedalus detector turns out to be

$$F_D = L_{NE}/L_M \tag{3}$$

where L_M is the measured radiance of a pixel.
Fig. 1 shows F_D as a function of a) the scan rate, averaged over 10 channels, and b) of the channels for a scan rate of 100 Hz (flight altitude of 300 m). It can be seen that F_D shows a relatively high value for the first channel, which is due to the decreasing sensitivity of the photodetector for shorter wavelengths. F_D remains at values below 2% for channels 2 to 10. The increase of F_D with increasing scan rate is mainly due to the decreasing exposure time. As a bulk value, F_D averaged over all scan frequencies and channels at a radiance of $L_M = 20\ Wm^{-2}\mu m^{-1}sr^{-1}$ (which we found as a good estimation for radiances during our overflights) can be assumed to be the instrumental noise of the scanner:

$$\overline{F_D}(20\ Wm^{-2}\mu m^{-1}sr^{-1}) = \begin{cases} 5.8\% & : \text{ for Daedalus band 1} \\ 0.5\% & : \text{ for Daedalus bands 2 to 10.} \end{cases}$$

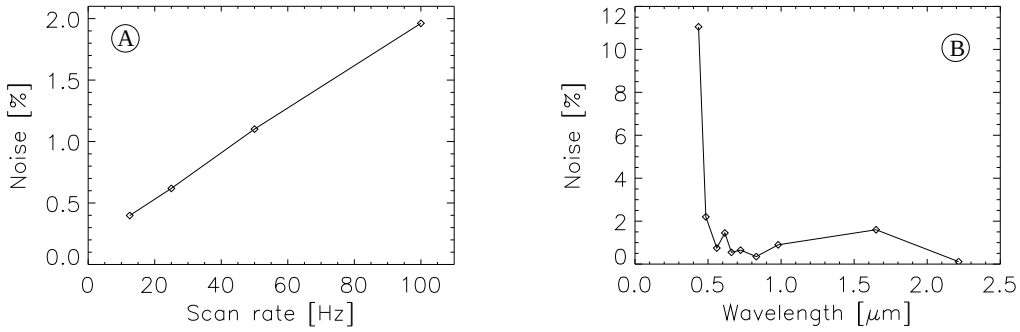

Figure 1: Relative values for instrumental noise of the Daedalus scanner for a radiance of $L_M = 20\ Wm^{-2}\mu m^{-1}sr^{-1}$. a) Dependence on scan rate (averages over channels 1 to 10) and b) Dependence on wavelength for 100 Hz scan rate ('worst case', the errors are smaller for lower scan rates).

3.2 Inaccurate knowledge of the atmospheric parameters

The acquisition of accurate information about local atmospheric parameters is a demanding experimental task. Often one can get only estimates of ground visibility, air pressure and humidity from 'nearby' weather stations. In our case we received such estimates from the meteorological station at the Nürnberg airport. In addition we used altitude profiles of air pressure, humidity and temperature measured at Amberg (50 km east of Nürnberg) by a radio sonde launch. In order to estimate the error caused by inaccurate knowledge of the local parameters, we made several runs with MODTRAN/SENSAT for different parameters. The illumination and viewing geometry was taken from one of our overflights and chosen to be typical for overflights at noon (altitude 300 m; heading 195°; sun zenith 39.34°; azimuth sun 173.47°, i.e. we are looking perpendicular to the flight direction). Assuming the aerosol type to be 'urban', we vary the visibility from 10 to 30 km for different atmospheres ('Midlatitude summer'and sonde data from Amberg). The calculation is done for all Daedalus channels. Fig. 2 shows the radiances for a ground reflectance of 10% when a) the visibility is varying between 10 km and 30 km (for sonde data of weatherstation Amberg), b) the atmosphere is varying between 'midlatitude summer' [McClatchey] and sonde data 'Amberg' for visibility of 15 km, c) shows the relative deviation when combining i) differences between 'Amberg' data at 15 and 20 km visibility and ii) differences between atmospheres 'midlat. summer' and sonde data 'Amberg' at 15 km visibility.

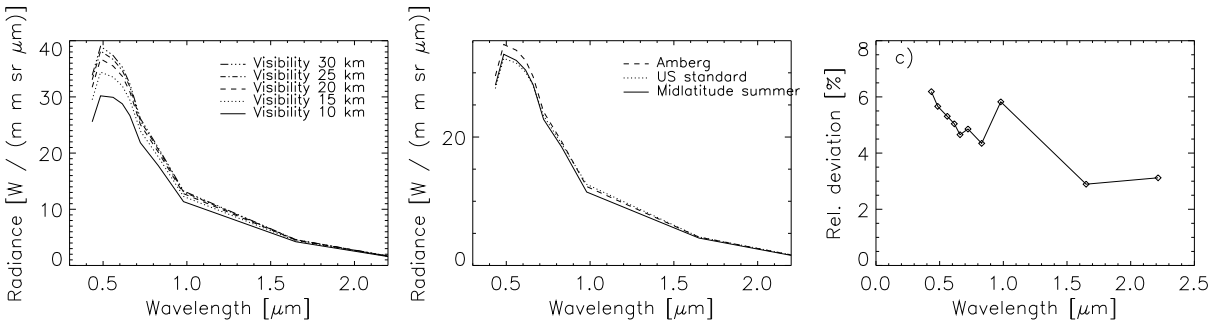

Figure 2: Differences in expected for a given ground reflectance of 10% at urban aerosol type a) visibility 10 to 30 km when using data 'sonde amberg' b) atmosphere 'midlatitude summer' or sonde 'Amberg' at visibility of 15 km c) estimated errors using deviation between 15 and 20 km at 'Amberg' data and b)

We believe that fig. 2 presents a lower limit to the systematic uncertainty caused by atmospheric conditions, because we had e.g. no way of checking the aerosol distribution (urban) for our application area.

3.3 Error propagation into reflectances

To calculate the reflectances from the Daedalus radiances, SENSAT models the radiances to be expected for several 'test reflectances'. The test reflectances, for which measured and modeled radiance agree is taken to be the measured reflectance ('inverse modeling' by look-up-table and interpolation). The laws of error propagation allow to calculate the error of the resulting reflectance when the errors of the used radiances are given (= results of chapters 3.1 + 3.2). Thus we found a relative reflectance error of 4.3 % (extrema are 2.1 % and 7.1%) averaged over reflectances of 5, 10, 15 and 20 % and all Daedalus channels. This value is to be considered as a lower limit of the pixel based reflectance for the reasons given. We also note that any further variability of the reflectance due to target inhomogenaities enters in most practical applications (mixed pixel and texture effects).

4 ACCURACY OF IRIS REFLECTANCE SPECTRA

Ground truth reflectance spectra were obtained by comparing the target region with a standard of known spectral characteristics ($BaSO_4$ and/or Spectralon). The spectroradiometer IRIS (made by GER, USA) is a dual field view instrument, allowing the measurement of the reflected radiance of the target and the reference to be made simultaneously. The IRIS was repaired and recalibrated by the manufacturer a month before our measurement. IRIS measurements were done with a $BaSO_4$-reference, spectral characteristics were determinend by intercalibration with a Spectralon-standard of known spectral reflectance [T. Kollewe, 1996]. Below, we estimate the error sources of this procedure.

4.1 Noise of IRIS-Detector.

Two field measurements (1997 data) made successively show differences caused by noise, mechanical and optical IRIS characteristics and small changes in illumination. By comparing the target (or reference) measurements, we obtain the noise of the detector. Fig. 3 shows the relative difference averaged over the target and reference channel. Its mean is $\approx$ 2.25%, except for atmospheric absorption bands and parts of the spectrum where the signal to noise ratio is low. Similar results were given in [T. Kollewe, 1996] for the 1994/1995 measurements of our group (1.5% noise and 1% error from mechanics).

4.2 Detector function.

Target- and reference-detector of the IRIS normally do not have the same charateristics. They have to be adjusted to each other by the detector function. Such a function is implemented in the software of the IRIS. Nevertheless we made four measurements with the $BaSO_4$ standard as target and reference simultaneously to obtain the 'current detector function' $f^t_{Det(\lambda)}$ (the ratio of target and reference measurement). Fig. 4 shows the four 'current detector functions'. Although the reference measurement is corrected by software, we see deviations from the expected ratio 'one'. Moreover we see differences between the ratios themselves (in the infrared), especially between the measurements which were made in the morning and those which were made past

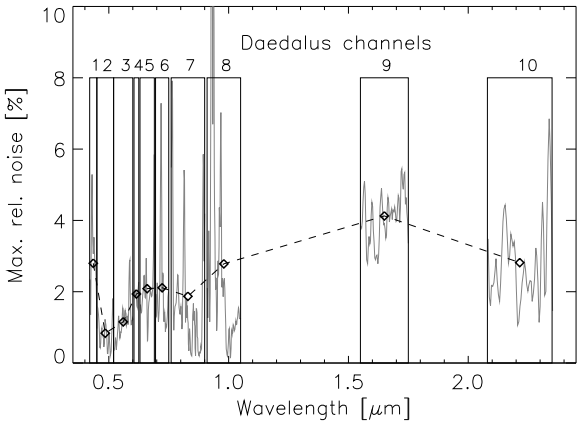

Figure 3: Maximum relative noise of IRIS detector (gray line). The circles connected the by dashed line show the mean values from IRIS noise averaged within the respective bands of the Daedalus detector.

10 UT. This may be caused by transporting the IRIS during the day to reach the differents target areas (see section 2.1).

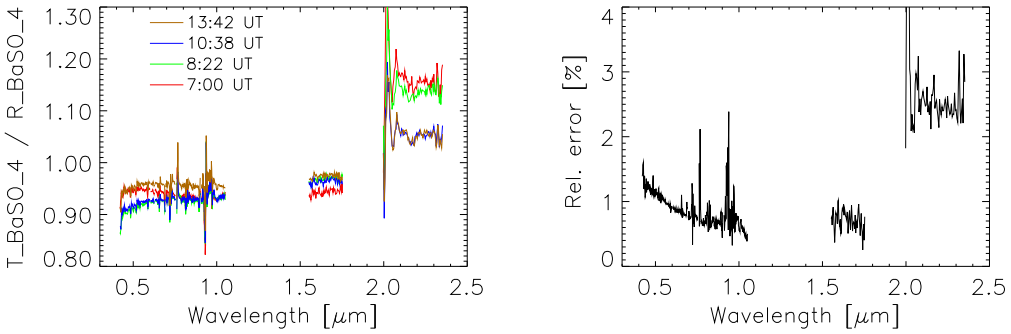

Figure 4: Comparisation of target and reference measurement (both $BaSO_4$). The left figure shows the ratios $f^t_{Det(\lambda)}$ between target and reference for different times t. The right figure shows the relative deviation from average.

The relative reflectance spectra $\rho_{rel}(\lambda)$ (ratio of target $T(\lambda)$ and reference measurement $R(\lambda)$) were divided by the simultaneously measured 'current detector function' $f_{Det(\lambda)}$.

$$\rho_{rel}(\lambda) = \frac{T(\lambda)}{R(\lambda)} \cdot \frac{R_{\mathrm{BaSO_4}}(\lambda)}{T_{\mathrm{BaSO_4}}(\lambda)} = \frac{T(\lambda)}{R(\lambda)} \cdot \frac{1}{f_{\mathrm{Det}(\lambda)}} \tag{4}$$

The errors were computed by gaussian error propagation. The error of $f_{\mathrm{Det}}(\lambda)$ was determined by quadratically adding the noise and the term $\sigma^2_{\mathrm{Timediff}}$, which takes the shift in the detector function (see right graphic of fig. 4) into account.

4.3 Calibration with reference standard.

In order to obtain absolute reflectance spectra, we calibrated the relative reflectance spectra $\rho_{rel}(\lambda)$ by comparison of a $BaSO_4$ and a Spectralon measurement ($T^0_{\mathrm{BaSO_4}}(\lambda)$, $T^0_{\mathrm{Spectralon}}(\lambda)$), both made with the target channel of IRIS (minimal time difference between both measurements, constant illumination was verified by an independent Pyranometer measurement). Absolute reflectance spectra $\rho_I(\lambda)$ are then given by:

$$\rho_I(\lambda) = \rho_{rel}(\lambda) \cdot \frac{T^0_{\mathrm{BaSO_4}}(\lambda)}{T^0_{\mathrm{Spectralon}}(\lambda)} \cdot \rho_{\mathrm{Spectralon}}(\lambda) \qquad , \tag{5}$$

where $\rho_{\mathrm{Spectralon}}(\lambda)$ is the known absolute reflectance of our Standard [Labsphere Inc., 1994].

4.4 Conversion of spectra into Daedalus channels.

IRIS reflectance spectra have a higher spectral resolution than the Daedalus spectra. To compare them, we averaged the IRIS reflectance spectra over the spectral bands of the Daedalus detector. Measurements for some target areas were made several times. We averaged them to take target inhomogeneity and changes in solar zenith angle (BRDF effects) into account.

Overall reflectance accuracy of IRIS from noise, detector function and calibration with reference standard is on average 3.2 % (does not exceed 5.5 %) in the wavelength region of Daedalus channels 1 to 8 and 6.6 % (does not exceed 8.0 %) in the wavelength region of Daedalus channels 9 to 10.

5 RECALIBRATION OF DAEDALUS DATA

To get rid of systematic errors, we performed a linear transformation from Daedalus into IRIS spectra by the least squares method. Marking the Daedalus-reflectances of the ground areas for band n by $x_{i,n}$ with error $\sigma_{x_{i,n}}$ and the analog IRIS measurements by $y_{i,n}$ with error $\sigma_{y_{i,n}}$, we minimized (varying the parameters a_n and b_n)

$$S = \sum_{i=1}^{N} \frac{\left[y_{i,n} - (a_n + b_n x_{i,n})\right]^2}{\sigma^2_{y_{i,n}} + b_n^2 \sigma^2_{x_{i,n}}} \qquad \mathrm{N:\ number\ of\ spectra\ used\ for\ recalibtation} \tag{6}$$

for each band. The transformed Daedalus spectra ρ are given by

$$\rho = b_n \cdot \rho_D + a_n \qquad n = 1 \text{ to } 10 \text{ for the bands of Daedalus} \tag{7}$$

The initial Daedalus reflectance spectra ρ_D were determined using the sonde data from weather station Amberg, the aerosol typ 'urban' of MODTRAN and a visibility of 15 km. Daedalus spectra used for recalibration were averaged over 5×5 pixel to be sure that the place of IRIS measurement is found. Moreover we corrected image data for adjacency effects (see section 5.1) and determined uncertainty in image data because of the target inhomogeneity and because of differences in angles of illumination and observation of the calibration targets(BRDF effects).

5.1 Adjacency effects

For targets of small size (size less then 7×7 pixels) and at the edges of larger targets the observed radiance is influenced by adjacent pixels. Especially for targets of low reflectance surrounded by high reflective materials (for example a water target surrounded by vegetation or asphalt next to a lawn as given at the airport), the surrounding contributions to the measured radiance are not negligable [Richter, 1996]. Comparing image data of the airport area with and without correction for adjacency ([Richter, 1992], [Hepp-94]) we found the change in reflectance is less then 1% for $\approx$ 50% of the image pixels and less than 7% for $\approx$ 90% of the image pixels. The number of pixels with changes in reflectance greater than 20% is about 1.5% . This shows that correction for adjacency is necessary.

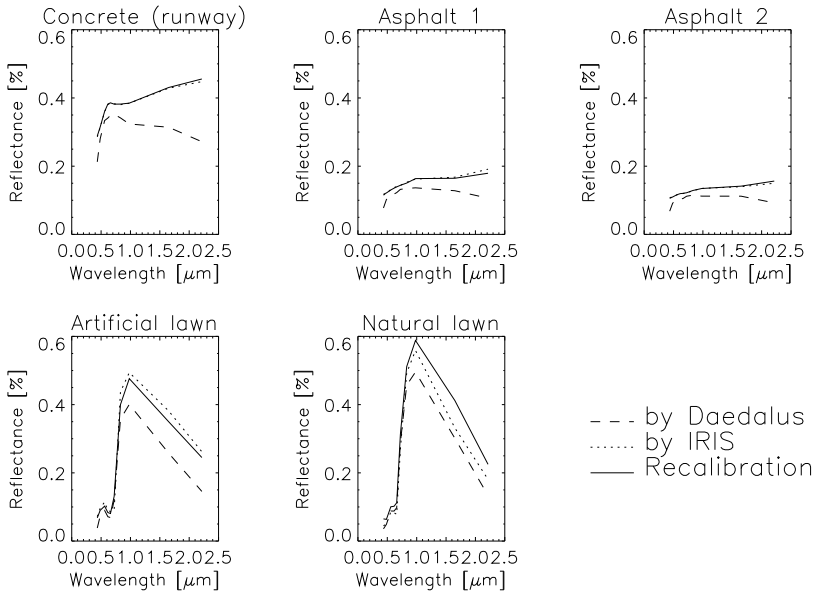

Figure 5: Comparision of Daedalus and IRIS spectra before and after recalibration. Surfaces were concrete, 2 $\times$ asphalt, artificial lawn and natural lawn (from top left to buttom right)

5.2 Inhomogeneity of the targets

The variability σ_M of a signal L_M measured by the airborne Daedalus-scanner, has two main sources, the intrumental noise of the scanner σ_N and the natural variability of the target. The law of error-propagation allows to seperate these contributions.We analysed the ground truth targets and seperated the natural variability. It turns out, that the relative lies at 5.5 % on average.

5.3 Different angles of illumination or observation of the calibration targets

The reflection of real surfaces often does not meet the Lambertian assumption, i.e. the intensity of the reflected radiance is not a simple function of the cosine of the incident irradiance. It must be described by the **Bi**directional **R**eflectance **D**istribution **F**unction [symbol: f_r; unit: 1/sr] as defined by [Nicodemus, 1970]. The BRDF is a function of the angles of incidence and reflection and of the wavelength. Therefore we may obtain different reflectances because of (a) time differences between the ground measurements and the overflights which cause different illumination angles and (b) off-nadir viewing of the Daedalus scanner (see table 1).

The BRDF of some artificial surfaces (for example concrete or roof coverings) can be described by an empirical function [Meister et al., 1996]. Using the parameters for concrete ([Meister et al., 1996]) and asphalt ([Monno, 1998]) we can estimate the difference in the reflectance between an IRIS ground measurement and the Daedalus measurement. The difference is caused by BRDF effects.

Table 1 shows the BRDF $f_r^{\theta_r=0^\circ}$ at nadir viewing (geometry of the IRIS measurements) and the BRDF f_r of the Daedalus viewing geometry of the three target areas used for recalibration for the different illumination and viewing angles (sun zenith θ_i, zenith viewing direction θ_r and relative azimuth angle ν). Relative deviation remains below 2 % for viewing zenith angles below 10°. For special illumination geometry (extreme off-nadir viewing and in direction of forward scattering) we see relative deviations up to 14 %.

TA	Overflight [time UT]	θ_i [°]	θ_r [°]	ν [°]	$f_r^{\theta_r=0°}$ $\left[10^{-2}\frac{1}{\mathrm{sr}}\right]$	f_r $\left[10^{-2}\frac{1}{\mathrm{sr}}\right]$	σ [%]
1	07:27	61.4	3.9	98.8	6.526	6.519	- 0.11
2	07:27	61.4	2.6	81.2	2.755	2.766	0.41
5	07:11	63.9	15.8	84.7	2.537	2.715	7.00
1	10:23	40.8	36.3	149.1	6.798	6.941	2.10
2	10:23	40.8	33.4	149.1	4.234	3.646	-13.87
5	10:33	40.3	16.5	27.6	4.261	4.408	3.44
1	11:36	39.4	7.6	177.1	6.508	6.453	- 0.84
2	11:36	39.4	1.9	2.9	4.313	4.337	0.55
5	11:12	39.2	7.2	12.3	4.323	4.404	1.88

Table 1: Estimated BRDF f_r for different target areas TA (see section 2.1) for different viewing and illumination geometry. The three rows indicate three different overflights, see sec. 2.1
σ means relative deviation

5.4 Overall uncertainty

Errors of the coefficients a_n and b_n were determined using the Monte Carlo method by adding random noise to $y_{i,n}$ and $x_{i,n}$ in equation 6 (the noise had a gaussian distribution of width $\sigma_{x_{i,n}}$ resp. $\sigma_{y_{i,n}}$). For Daedalus reflectances of 5, 10, 15 and 20 % (typical in our images) we found a relative accuracy of σ_ρ/ρ = 11.0 % (average over channels and reflectances) for the corrected Daedalus spectra ρ.
Note: The calculated radiances from MODTRAN/SENSAT are not valid for inclined surfaces (missing 3D model of our testsite). So the given accuracy is only valid for non-inclined surfaces.

6 SUMMARY

Reflectance spectra of selected surfaces (concrete, asphalt, natural lawn, artificial lawn) were determined from airborne images (Daedalus AADS 1268 scanner) using the radiative transfer package MODTRAN/SENSAT and ground based reflectance measurements. For typical Daedalus reflectances (between 5 and 20 %) we estimated a lower limit of the relative accuracy of pixel based reflectances of 4.3 % on average. The average reflectance accuracy of IRIS ground based measurements is 3.9 %. Using the IRIS reflectances ρ_I, the Daedalus reflectances ρ_D can be recalibrated. After the recalibration the accuracy of Daedalus reflectance σ_ρ/ρ is 11.0 % on average. We consider this to be a conservative estimate of the reflectance accuracy which can be derived from Daedalus AADS 1268 sensor data for multipixel areas in the absence of detailed knowledge of atmospheric conditions beyond ground visibility, pressure and temperature.

Acknowledgement

We would like to thank our colleagues of our working group and the coworkers of the Dep. for Informatics for their support and fruitful discussion. The flight campaign was performed in collaboration with the German Aerospace Research Establishment (DLR), Oberpfaffenhofen, FRG. We acknowledge the contributions particularly of Volker Amman and Rudolf Richter from DLR. IRIS ground measurements were done in cooperation with the Bundesamt für Geowissenschaften und Rohstoffe in Hannover (BGR), FRG, particularly by Jürgen Ruder and Dr. Bannert from BGR.

References

[Anderson et al., 1995] Anderson G.P., Kneizys F.X., Chetwynd J.H., Wang J., Hoke M.L., Rothman L.S., Kimball L.M., McClatchey R.A., Shattle E.P., Clough S.A., Gallery W.O., Abreu L.W. and Selby J.E.A., 'FASCODE / MODTRAN / LOWTRAN : Present / Past / Future', Proceedings of the 18th Annual Review Conference on Atmospheric Transmission Models, June 6–8, 1995

[McClatchey] R. A., W. Fenn, J. E. A. Selby, F. E. Volz, J. S. Garing (1972): Optical Properties of the Atmosphere; *AFCRL Envirn. Res. Papers* **411**, 108pp.

[Hepp-94] T. Hepp, 1994. Erzeugung multispektraler Reflektanzbilder zur automatisierten Bildauswertung, diploma thesis, CENSIS-REPORT-10-94, Universität Hamburg, II. Institut für Experimentalphysik, FRG.

[T. Kollewe, 1996] T. Kollewe, 1996. Vergleich multispektraler Flugzeugscanneraufnahmen mit Reflektanzmessungen am Boden, diploma thesis, CENSIS-REPORT-17-96, Universität Hamburg, Universität Hamburg, FRG.

[M. Kollewe et al., 1996] M. Kollewe, J. Bienlein, T. Kollewe, H. Spitzer, Comparison of Multispectral Airborne Scanner Reflectance Images With Ground Surface Reflectance Measurements, Second International Airborne Remote Sensing Conference and Exhibition, San Francisco 1996, vol III, p. 220-228, ERIM Ann Arbor 1996.

[Labsphere Inc., 1994] Calibration certificate SRT-50-120, Report No. 12611-D, Labsphere Inc., P.O.Box 70, North Sutton, NH 03260, Nov. 1994

[Meister, 1996] G. Meister, 1996. Messung der spektralen Reflexionsfunktion (BRDF) ausgewählter Oberflächen bei natürlicher Beleuchtung, diploma thesis, Universität Hamburg, II. Institut für Experimentalphysik, CENSIS-REPORT-18-96.

[Meister et al., 1996] G. Meister, R.Wiemker, J. Bienlein, H. Spitzer, In Situ Measurements of Selected Surface Materials to Improve Analysis of Remotely Sensed Multispectral Imagery, Proceedings of the XVIII. Congress of the International Society for Photogrammetry and Remote Sensing ISPRS, 1996, Vienna, volume XXXI part B7 of International Archives of Photogrammetry and Remote Sensing, p.493 - 498, 1996.

[Monno, 1998] R. Monno, University of Hamburg, II. Institut für Experimentalphysik, privat communication, 1998.

[Nicodemus, 1970] F.E. Nicodemus, 1970. Reflectance Nomenclature and Directional Reflectance and Emissivity, Applied Optics, 9 (6), pp. 1474-1475.

[Richter, 1992] R. Richter, Radiometrische Auslegung von Sensoren und quantitative Auswertung von Fernerkundungsdaten im optischen Spektralbereich, DLR-FB 9201, (1992)

[Richter, 1994] R. Richter, 1994. Model SENSAT-5 Sensor-Atmosphere-Target, DLR-IB 552-01/94, DLR- Institute for Optoelectonis, Wessling/Munich, FRG.

[Richter, 1996] R. Richter, On the in-flight absolute calibration of high spatial resolution spaceborne sensors using small ground targets, Int. J. Remote Sensing, 1997, Vol.18, No.13, pp.2817-2833.

[Wiemker et al., 1997] Wiemker R., Speck A., Kulbach D., Spitzer H., Bienlein J., 'Unsupervised Robust Change Detection on Multispectral Imagery Using Spectral and Spatial Features', Proceedings of the Third International Airborne Remote Sensing Conference and Exhibition, Copenhagen, July 1997, vol. I, p.640-647. ERIM, Ann Arbor 1997.